PARAMETRIC TROMBONE SYNTHESIS BY COUPLING DYNAMIC LIP VALVE AND INSTRUMENT MODELS

Tamara Smyth, Frederick Scott
School of Computing Science, Simon Fraser University
tamaras@cs.sfu.ca, fss3@cs.sfu.ca

ABSTRACT

In this work, a physics-based model of a trombone coupled to a lip reed is presented, with the parameter space explored for the purpose of real-time sound synthesis. A highly configurable dynamic lip valve model is reviewed and its parameters discussed within the context of a trombone model. The trombone model is represented as two separate parametric transfer functions, corresponding to tapping a waveguide model at both mouthpiece and bell positions, enabling coupling to the reed model as well as providing the instrument's produced sound. The trombone model comprises a number of waveguide filter elements—propagation loss, reflection at the mouthpiece, and reflection and transmission at the bell—which may be obtained through theory and measurement. As oscillation of a lip reed is strongly coupled to the bore, and playability strongly dependent on the bore and bell resonances, it is expected that a change in the parameters of one will require adapting the other. Synthesis results, emphasizing both interactivity and high-quality sound production are shown for the trombone in both extended and retracted positions, with several example configurations of the lip reed.

1. INTRODUCTION

In this work, a physics-based model of a trombone is presented, suitable for real-time sound synthesis, emphasizing both interactive control parameters and high-quality sound production.

The sound produced by the trombone may be seen as the coupling of the input pressure from the lips (the product of the volume velocity and the bore opening's characteristic impedance) with the instrument bore and bell—a convolution of the lip-valve signal and the trombone impulse response.

In previous work [1], a parametric model of the trombone's transfer function is obtained in two positions: one tapped at the position of the mouthpiece and the other outside the bell. The former may be coupled to a lip-valve model, providing feedback of bore resonances and the pressure difference across the lip valve (required for dynamic models in which the bore pressure influences the behaviour of the vibrating lips [2]), while the latter may be convolved with the lip-valve signal to provide the instrument's produced sound.

The instrument body model, discussed in Section 2, employs a measurement and a processing technique from previous work [3, 1], whereby waveguide elements are estimated from several measurements of the system's impulse response, with the system having incrementally varying boundary conditions to allow for the isolation and estimation of filter transfer functions. The work in [1] focused on obtaining waveguide elements for the trombone instrument model, while the work here focuses on coupling this instrument to a generalized reed model.

The parameter space of a dynamic lip valve model is explored when coupled to a trombone synthesis model. To provide context and present parameters, the valve model is discussed in Section 3. Coupling to the trombone model with and without a mouthpiece is discussed in Section 4.

2. TROMBONE INSTRUMENT MODEL

It is well known that wave propagation in wind instrument bores may be modeled in one dimension using the waveguide structure shown in Figure 1, with a bi-directional delay line of length M samples accounting for the acoustic propagation delay in the cylindrical and/or conical tube section of a given length, and filter elements $\lambda(z)$, $R_0(z)$, $R_L(z)$ and $T_L(z)$, accounting for the propagation loss, reflection at the mouthpiece, and open-end reflection and transmission occurring at the position of the bell, respectively, all of which may contain delays, poles or "long-memory" information on the acoustics of non-cylindrical and non-conical bore sections [4, 5]. That is, the approach shown in Figure 1 separates an instrument horn into its cylindrical/conical and flared sections, with lumped filters accounting for the reflection and transmission of the flared bell—properties which contribute significantly to the instrument's characteristic resonances.

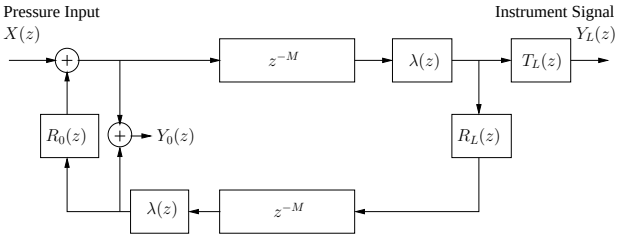

Figure 1. Waveguide model of a cylindrical tube with commuted propagation loss filters $\lambda(z)$, open-end terminating reflection and transmission filters $R_L(z)$ and $T_L(z)$ respectively, and a reflection filter $R_0(z)$ at the (effectively) closed end termination corresponding to the position of the mouthpiece. Two instrument transfer functions (1) and (2) are developed for observation points yielding $Y_0(z)$ and $Y_L(z)$, corresponding to the bore base and the instrument output, respectively, in response to input pressure $X(z)$.

For synthesis applications, it is useful to tap the signal flow diagram in Figure 1 at two different positions, producing pressures $Y_0(z)$ and $Y_L(z)$ in response to input pressure $X(z)$. This yields two separate instrument transfer functions which may be used to couple the instrument to a dynamic lip reed model at the mouthpiece, as well as produce the instrument's sound output at the bell.

As shown in [1], ignoring the time-varying component in the mouthpiece, the global transfer function $H = Y_0/X$ at the bore base is given in the z-domain by

$$H(z) = \frac{Y_0(z)}{X(z)} = \frac{1 + \lambda^2(z)R_L(z)z^{-2M}}{1 - \lambda^2(z)R_L(z)R_0(z)z^{-2M}}, \quad (1)$$

where $\lambda(z)$ is the propagation loss and $R_0(z)$ and $R_L(z)$ are the reflection functions describing the boundaries at the position of mouthpiece and bell, respectively, and where $Y_0(z)$ is based on the power series expansion

$$\begin{aligned} Y_0(z) &= X(z)(1 + \lambda^2(z)R_L(z)z^{-2M}) \times \\ &\quad [1 + R_0(z)R_L(z)\lambda^2(z)z^{-2M} + \\ &\quad R_0(z)R_L(z)\lambda^2(z)z^{-2M} + ...]. \end{aligned}$$

Similarly, the global transfer function $G = Y_L/X$ at the instrument output (at the bell) is given in the z-domain by

$$G(z) = \frac{Y_L(z)}{X(z)} = \frac{T_L(z)\lambda(z)z^{-M}}{1 - \lambda^2(z)R_L(z)R_0(z)z^{-2M}}, \quad (2)$$

where $T_L(z)$ is the transmission function of the bell, and where $Y_L(z)$ is based on the power series expansion

$$\begin{aligned} Y_L(z) &= X(z)T_L(z)\lambda(z)z^{-M} \times \\ &\quad [1 + R_0(z)R_L(z)\lambda^2(z)z^{-2M} + \\ &\quad R_0(z)R_L(z)\lambda^2(z)z^{-2M} + ...]. \end{aligned}$$

Expressing the instrument model in this way conveniently allows for the alternate equivalent representation shown in Figure 2, whereby the input pressure $x(t) = Z_0U(t)$, the product of the characteristic impedance Z_0 and volume flow $U(t)$ derived from a reed model in response to a blowing pressure $p_m(t)$, is convolved with instrument impulse responses $h(t)$ and $g(t)$, the inverse Fourier transforms of the frequency responses corresponding to (1) and (2), respectively. Implementing the model in this way, allows for extensions of the trombone instrument model that are not bounded by the physical constraints of the waveguide model, the basis for convolutional synthesis in [6],

2.1 Trombone Model Parameters

Whether using waveguide or convolutional synthesis implementation, the model described by (1) and (2) comprise several filter elements describing the acoustic characteristics of the system:

- **The delay of M samples** accounts for the acoustic propagation delay in the bore, the value typically being set according to the bore's effected length or the desired sounding pitch.
- **Propagation/wall losses** $\lambda(\omega)$ are well described theoretically [7, pp. 193-196], with a parametric filter described in [8], allowing for real-time changes according to tube size and length.

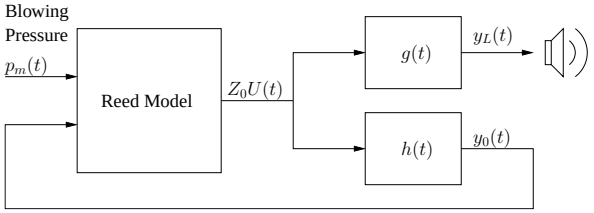

Figure 2. A convolutional synthesis approach to the signal flow diagram shown in Figure 1, with signals $h(t)$ and $g(t)$ being the impulse responses of the instrument tapped at the positions $y_0(t)$ and $y_L(t)$, the inverse transforms of (1) and (2), respectively. The input pressure is the product of the characteristic (wave) impedance Z_0 at the mouthpiece and the volume flow $U(t)$, a signal generated by a reed model in response to a blowing pressure $p_m(t)$.

Part	Length (cm)	Radius (cm)
t. inner slide (1)	70.8	0.69
t. outer slide, ext. (2)	53	0.72
slide crook (3)	17.7	0.74
b. outer slide, ext. (4)	53	0.72
b. inner slide (5)	71.1	0.69
gooseneck (6)	24.1	0.71
tuning slide (7)	25.4	0.75,1.07
bell flare (8)	56.7	1,10.8

Table 1. Trombone tubular sections (numbers correspond to parts in Figure 3) and dimensions, including top (t.) and bottom (b.) inner and outer slides, retracted and extended (ext.).

- **The reflection and transmission at the bell, $R_L(z)$ and $T_L(z)$**, respectively, may be derived either from a computational model or from measurement, with the former emphasizing parametrization and ability to change the bell contour during performance, and with the latter offering assumed greater accuracy. Because the trombone bell is not expected to change during performance, and because it disassembles easily from the trombone bore, its reflection and transmission functions may be estimated using the measurement technique described in [1].
- **The reflection at the mouthpiece position** $R_0(\omega)$. As this is expected to change during performance with the vibrating lips changing both the mouthpiece volume and the opening to the bore, it is not suitably obtained using the methods described in [3, 1], and is better developed within the context of coupling with the dynamic lip reed model discussed in Section 4.

A complete trombone (mouthpiece omitted), is shown in Figure 3, with corresponding trombone components and dimensions provided in Table 1. Figure 3 shows an interior view of the complete trombone in both retracted and extended positions, producing bores with effective lengths of 209.1 cm and 315.1 cm respectively, with asterisks showing possible cylindrical junctions that may or may not be considered depending on the desired level of accuracy (they are omitted here). Trombone components 1-7 in Figure 3 are modeled as a single cylindrical waveguide section, following dimensions in Table 1 for appropriate delay length

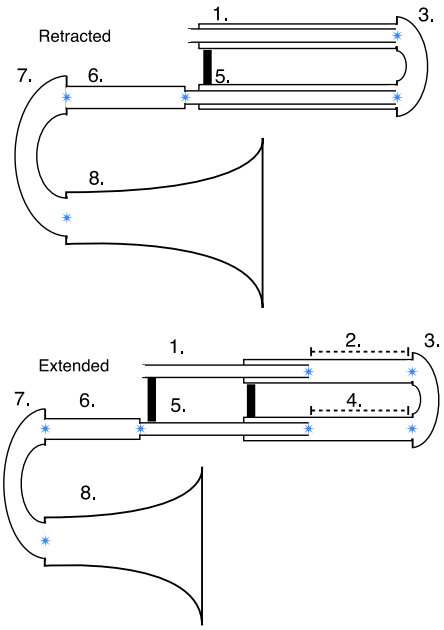

Figure 3. Interior view of trombone, in both fully retracted and fully extended positions, showing assembly of components from Table 1.

and average radius, the parameters required for the propagation loss model described in [8].

3. LIP VALVE MODEL

In reed instruments, input air pressure from the lungs/mouth controls the oscillation of a valve by creating a pressure difference across it's surface. The oscillation of a "blown open" valve, a typical characterization of the trombone's lip reed [9], is strongly coupled to the bore, making playability (and thus a *regular* non-chaotic oscillation of reed), highly dependent on the bore and bell resonances. It is expected, therefore, that the configuration and parameter values of a dynamic reed model would be dependent on the instrument to which it is coupled, as well as any changes-such as an extending slide—occurring during performance.

Here, the generalized pressure-controlled valve model, first introduced in [2], is reviewed to provide context for the configuration and playing control values explored within the context of the trombone model (described in Section 2).

3.1 Generalized Pressure Control Valve

The generalized parametric model of a pressure-controlled valve [2], affords the user the ability to design a continuum of reed configurations, including "blown-open", "blown-closed", and the "swinging door", typically seen in wind and vocal systems, simply by setting model parameters.

Figure 4 illustrates one model of oscillation of the blown open configuration, with the displacement of the valve being given by its angle θ from the vertical axis. The valve classification is determined in part by its initial position θ_0 (its equilibrium position in the absence of flow), and in part by the use of an optional *stop*—a numerical limit placed to

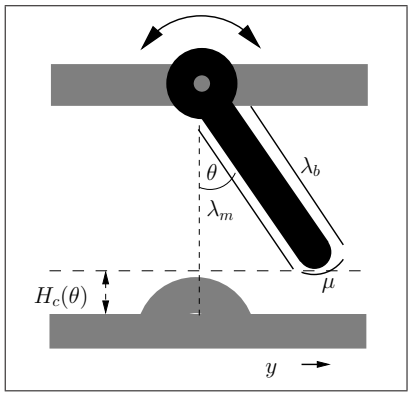

Figure 4. The blown open configuration of the generalized valve model, showing geometric parameters λ_m, the length of the valve that sees the mouth pressure, λ_d, the length of the valve that sees the valve's downstream pressure, and μ, the length of the valve that sees the flow. Changing these parameters will change the corresponding component forces of the overall driving force $F = F_m + F_b + F_U$.

constrain the range of θ. In Figure 4, the stop is placed at the center vertical axis, $\theta = 0$. If a stop is placed in the channel, the configuration is further determined by the initial equilibrium position of the valve θ_0: an initial position to the left of the stop, at $\theta_0 < 0$, will cause the reed to *blow closed*, while an initial position to the right of the stop, $\theta_0 > 0$, will cause the reed to *blow open*. The trombone classification, typically considered to be *blown open*, is implemented with $\theta_0 > 0$ plus a stop.

The valve channel area is critical to the volume flow and resulting sound of the instrument. As the reed angle θ changes, the valve opening area A changes according to channel height H_c

$$A(\theta) = wH_c(\theta), \tag{3}$$

where w is the width of the channel. The height of the valve channel in the presence of an oscillating reed may be specified by the function $H_c(\theta)$, a number of possible functions depending on choice of valve. To approximate channel area of a lip reed, the height function may be set to

$$H_c(\theta) = 1 - \cos\theta. \tag{4}$$

The geometry of the valve may be further specified by setting the effective length of the reed that sees the mouth pressure λ_m, the reed length that sees the bore pressure λ_b, and the reed length that sees the flow, given by μ (see Figure Figure 4). These variables have an audible effect on the overall driving force acting on the reed, given by F in (5), and can be seen as offering finer control of embouchure.

Once the valve is set into motion, the value for θ is determined by the second order differential equation

$$m\frac{d^2\theta(t)}{dt^2} + m2\gamma\frac{d\theta(t)}{dt} + k(\theta(t) - \theta_0) = F, \tag{5}$$

where m is the effective mass of the reed, γ is the damping coefficient, k is the stiffness of the reed, and F is the overall driving force acting on the reed, a function of the mouth and bore pressure, and flow in contact with the reed. The frequency of vibration for this mode is given by $\omega_v = \sqrt{k/m}$.

Discretization, equivalent to applying a bilinear transform, yields the transfer function in the z-domain

$$\frac{\theta(z)}{F(z)+k\theta_0} = \frac{1+2z^{-1}+z^{-2}}{a_0+a_1z^{-1}+a_2z^{-2}}, \tag{6}$$

and the corresponding difference equation

$$\begin{aligned}\theta(n) &= [F_k(n)+2F_k(n-1)+F_k(n-2)- \\ &\quad a_1\theta(n-1)-a_2\theta(n-2)]/a_0,\end{aligned} \tag{7}$$

where $F_k(n) = F(n)+k\theta_0$, and

$$\begin{aligned}a_0 &= m\alpha^2+mg\alpha+k,\\ a_1 &= -2(m\alpha^2-k),\\ a_2 &= m\alpha^2-mg\alpha+k,\end{aligned}$$

and $\alpha = 2/T$, where T is the sampling period, and $g = 2\lambda$. Since pole frequencies are well below the Nyquist limit (half the sampling rate), there is no need for pre-warping.

The force driving the reed F is equal to the sum of the forces acting on the reed, $F = F_m+F_b+F_U$, where $F_m = w\lambda_m p_m$ is the force acting (in the positive θ direction) on the surface area $\lambda_m w$, $F_b = -w\lambda_b p_b$, is the force acting (in the negative θ direction) on the surface area $\lambda_b w$, and F_U is the force applied by the flow (which forces the reed open) given by

$$F_U = \text{sign}(\theta)w\mu\left(p_m - \frac{\rho}{2}\left(\frac{U(t)}{A(t)}\right)^2\right). \tag{8}$$

As can be seen by (8), the total force driving the reed is dependent on the valve classification, since the sign of θ is determined by its limits.

The differential equation governing air flow through the valve, fully derived in [10], is given by

$$\frac{dU(t)}{dt} = (p_m-p_b)\frac{A(t)}{\mu\rho} - \frac{U(t)^2}{2\mu A(t)+U(t)T}. \tag{9}$$

where p_m is mouth pressure, p_b is the bore pressure (see discussion in the following section), $A(t)$ is the cross sectional area of the valve channel, and μ is the length of reed that sees the flow. Equation (9) is used to update the flow U every sample period (given by the inverse of the sampling rate).

There are, therefore, three variables that evolve over time in response to an applied mouth pressure p_m: the displacement of the reed θ (determined using 7), the flow U, determined using the update given by (9), and the pressure at the base of the bore p_b, obtained using either waveguide synthesis or a low-latency convolution [11], as mentioned in Section 2.

Since the contour of the bore and bell to which the reed is connected strongly influences the reed's oscillation, the valve model must have a new configuration and set of parameter values for each new instrument application.

4. COUPLING LIP AND INSTRUMENT MODELS

Connecting the lip model to the instrument can be done in two ways: The first would be more simplistic and would omit a mouthpiece. The second would be to introduce a new element, the mouthpiece (described below), to account for the resonance created by the mouthpiece's cup volume and its backbore constriction.

4.1 Mouthpiece Model

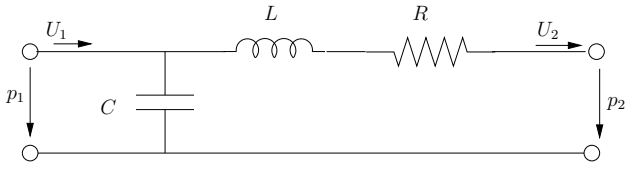

Figure 5. The system diagram for the mouthpiece model. The cup volume is represented by the capacitor, and the attached narrow constriction is modeled as a series inertance L and dissipative element R, which accounting for wall losses.

Improvements to the trombone model may by made by including the effects of a mouthpiece, an important structural element to the complete trombone instrument, which introduces a characteristic resonance determined by the combination of the cup volume and constriction diameter of the backbore [7]. As shown in [7, 12, 13] (and others), the mouthpiece may be modeled by the equivalent electrical circuit shown in Figure 5. The mouthpiece consists of a cup having a volume V, and presents an acoustic compliance C given by

$$C = \frac{V}{\rho c^2}, \tag{10}$$

where ρ is the air density and c is the velocity of sound in air. The cup is followed by a constricted passage before entering into the wider trombone bore, with the constriction behaving as a series inertance (inductance in electrical terms) given by

$$L = \frac{\rho l_c}{S_c}, \tag{11}$$

where l_c is the length and S_c is the cross-sectional area of the constriction. The dissipative element R in series with this inertance represents viscous and thermal losses. Its value for the mouthpiece has been obtained through experiment in [14].

Inserting a mouthpiece between the reed and bore models requires a new expression for the volume flow entering the bore (it is no longer that coming directly from the lips), as well as a new expression for the downstream pressure used when in the dynamic lip reed model (it is no longer the bore base pressure). These quantities are termed $U_2(t)$ and $p_1(t)$, respectively, in Figure 5.

The mouthpiece model provides a volume flow $U_2(t)$ into the bore and a pressure $p_1(t)$ in the mouthpiece, in response to a volume flow $U_1(t)$ entering the mouthpiece (generated by the lip reed model) affixed to the instrument having a pressure of $p_2(t)$ at the bore base.

Taking the Laplace transform of the differential equations describing the mouthpiece model in Figure 5 leads to the system's frequency domain input-output matrix

$$\begin{bmatrix}U_1(s)\\ p_1(s)\end{bmatrix} = \begin{bmatrix}s^2LC+sRC+1 & sC\\ sL+R & 1\end{bmatrix}\begin{bmatrix}U_2(s)\\ p_2(s)\end{bmatrix}, \tag{12}$$

which may be rearranged and discretized to yield expressions for U_2 and p_1 in response to U_1 and p_2, given in the z-domain as

$$U_2(z) = \frac{U_1(z)(1+2z^{-1}+z^{-2}) - C\alpha p_2(z)(1-z^{-2})}{a_{m0}+a_{m1}z^{-1}+a_{m2}z^{-2}}, \tag{13}$$

Quantity	Variable	Value
radius of exhaust	a	8mm
valve width	w	2.3 mm
valve length	$\lambda_m = \lambda_b$	23.2 mm
valve mass	m	.3g
valve thickness	μ	6mm
initial displacement	θ_0	0.01mm
mouthpiece volume	V	$5 \times 10^{-6}\text{m}^3$
mouthpiece choke length	l_c	48 cm
mouthpiece choke radius	a_c	4.5 mm

Table 2. Example valve parameters values.

where

$$\begin{aligned} a_{m0} &= LC\alpha^2 + RC\alpha + 1 \\ a_{m1} &= -2(LC\alpha^2 - 1) \\ a_{m2} &= LC\alpha^2 - RC\alpha + 1 \end{aligned}$$

and

$$p_1(z) = \frac{U_2(z)(b_0 + b_1 z^{-1}) + p_2(z)(1 + z^{-1})}{1 + z^{-1}}, \quad (14)$$

where

$$b_0 = L\alpha + R \quad \text{and} \quad b_1 = -L\alpha + R,$$

and $\alpha = 2/T$, where T is the sampling period. The corresponding difference equations are given by

$$\begin{aligned} U_2(n) &= [U_1(n) + 2U_1(n-1) + U_1(n-2) - \\ &\quad C\alpha\,(p_2(n) - p_2(n-2)) - \\ &\quad a_1 U_2(n-1) - a_2 U_2(n-2)]/a_0, \end{aligned}$$

and

$$\begin{aligned} p_1(n) &= b_0 U_2(n) + b_1 U_2(n-1) + \\ &\quad p_2(n) + p_2(n-1) - p_1(n-1). \end{aligned}$$

Again, as for the case of discretizing the valve displacement, no pre-warping is required.

5. CONCLUSIONS

In this work, a previously presented trombone model is augmented with a mouthpiece and coupled to a dynamic lip reed model, to explore the resulting parameter space as well as experiment with it's synthesis capabilities. Example outputs of the model are shown in Figure 6 and Figure 7, showing the effects of the mouthpiece, with the slide both retracted and extended, in both time and frequency domains, using parameter values in Table 2. To illustrate the effects of the mouthpiece, all other parameters remain the same. It should be noted however, that in actual practice, a change in the instrument parameter will likely require an adapted change in the lip reed as well.

Acknowledgments

The authors would like to acknowledge the support of the Natural Sciences and Engineering Research Council of Canada (NSERC) and the Canada Council for the Arts (CCA) through the Discovery and New Media Initiative programs.

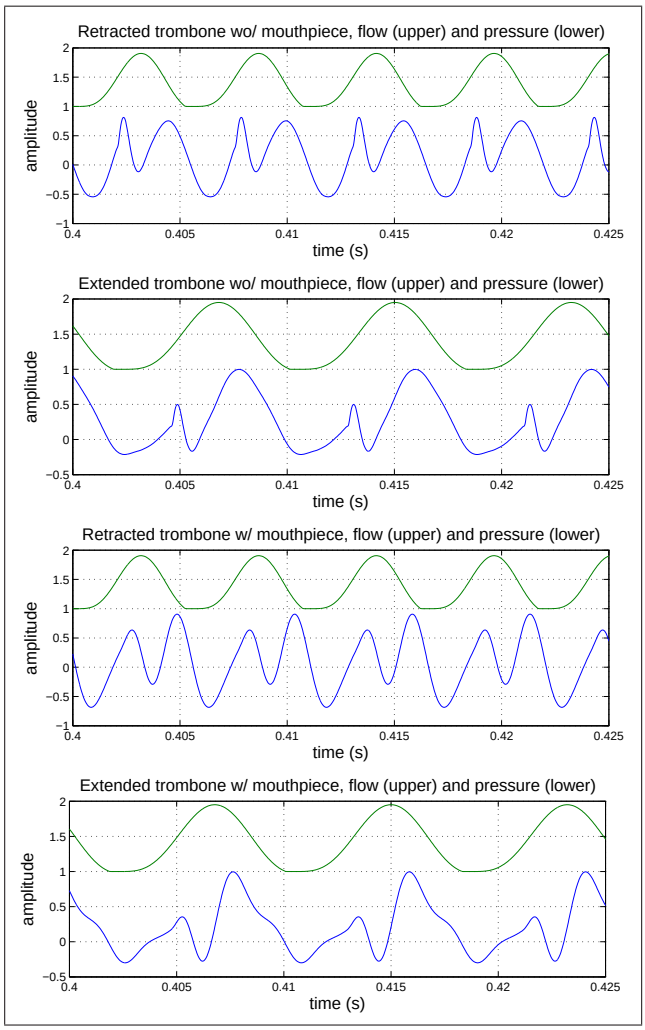

Figure 6. Synthesis examples using parameter values from Table 1 and Table 2, showing flow versus bell output pressure (produced sound) in a note's steady state, with slide in both retracted and extended positions, and with and without a mouthpiece.

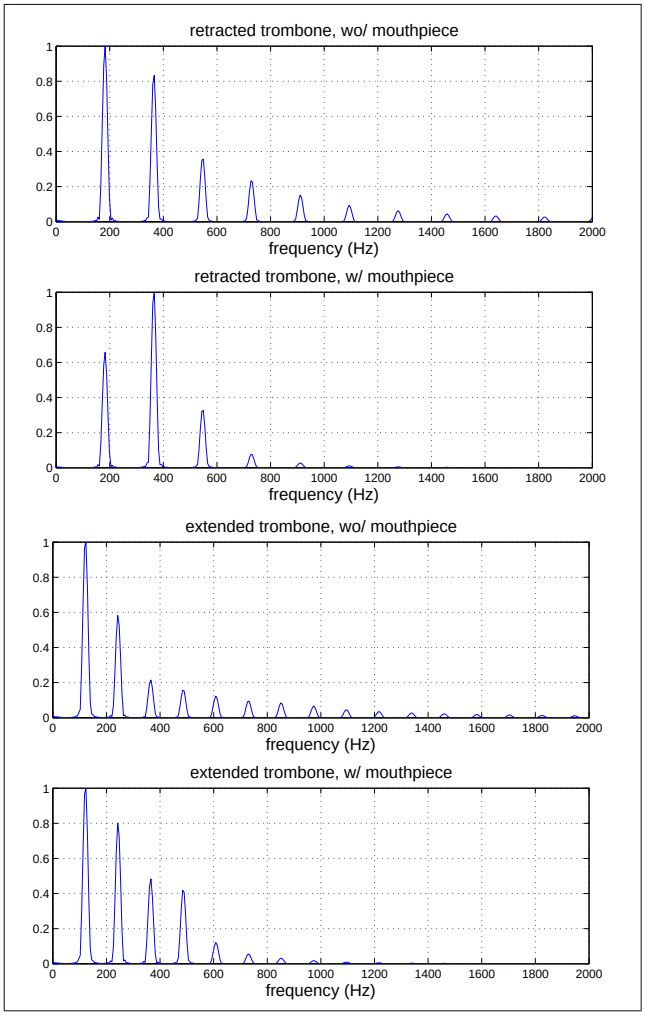

Figure 7. Synthesis examples from Figure 6, showing effects of the mouthpiece in the frequency domain

6. REFERENCES

[1] T. Smyth and F. S. Scott, "Trombone synthesis by model and measurement," *EURASIP Journal on Advances in Signal Processing*, vol. 2011, no. Article ID 151436, p. 13 pages, 2011, doi:10.1155/2011/151436.

[2] T. Smyth, J. Abel, and J. O. Smith, "A generalized parametric reed model for virtual musical instruments," in *Proceedings of ICMC 2005*. Barcelona, Spain: International Computer Music Conference, September 2005, pp. 347–350.

[3] T. Smyth and J. Abel, "Estimating waveguide model elements from acoustic tube measurements," *Acta Acustica united with Acustica*, vol. 95, no. 6, pp. 1093–1103, 2009.

[4] J. O. Smith, "Physical audio signal processing for virtual musical instruments and audio effects," http://ccrma.stanford.edu/˜jos/pasp/, December 2008, last viewed 8/18/2010.

[5] V. Välimäki, J. Pakarinen, C. Erkut, and M. Karjalainen, "Discrete-time modelling of musical instruments," *Report on Progress in Physics*, vol. 69, pp. 1–78, 2006.

[6] T. Smyth and J. Abel, "Convolutional synthesis of wind instruments," in *Proceedings of the IEEE Workshop on Applications of Signal Processing to Audio and Acoustics (WASPAA'07)*, New Paltz, New York, October 2007.

[7] N. H. Fletcher and T. D. Rossing, *The Physics of Musical Instruments*. Springer-Verlag, 1995.

[8] J. Abel, T. Smyth, and J. O. Smith, "A simple, accurate wall loss filter for acoustic tubes," in *DAFX 2003 Proceedings*. London, UK: International Conference on Digital Audio Effects, September 2003, pp. 53–57.

[9] N. H. Fletcher, "Autonomous vibration of simple pressure-controlled valves in gas flows," *Jounal of the Acoustical Society of America*, vol. 93, no. 4, pp. 2172–2180, April 1993.

[10] T. Smyth, J. Abel, and J. O. Smith, "The feathered clarinet reed," in *Proceedings of the International Conference on Digital Audio Effects (DAFx'04)*, Naples, Italy, October 2004, pp. 95–100.

[11] W. G. Gardner, "Efficient convolution without input-output delay," *Journal of the Audio Engineering Society*, vol. 43, no. 3, pp. 127–136, March 1995.

[12] M. van Walstijn, "Discrete-time modelling of brass and reed woodwind instruments with application to musical sound synthesis," Ph.D. dissertation, University of Edinburgh, 2002.

[13] B. Krach, S. Petrausch, and R. Rabenstein, "Digital sound synthesis of brass instruments by physical modeling," in *Proceedings of the International Conference on Digital Audio Effects (DAFx'04)*, Naples, Italy, October 2004.

[14] P. Dietz, "Simulation of trumpet tones via physical modeling," Master's thesis, Dept. of Electrical Engineering, Bucknell University, Lewisburg, USA, 1988.